proceedings

MDPI

Proceedings

Enhanced gut microbiota-produced propionate associates with neuroinflammation and cognitive impairment in a murine model of Alzheimer´s disease

Daniel Cuervo-Zanatta[1], Mariangel Irene-Fierro[2], Alberto Piña-Escobedo[1], Vicente Sánchez-Valle[2], Jaime García-Mena[1] and Claudia Perez-Cruz[2]*

[1] Genetics and Molecular Biology Department. Center for Research and Advanced Studies of the National Polytechnic Institute (CINVESTAV-IPN), Zacatenco Unit. 2508 National Polytechnic Institute Avenue. San Pedro Zacatenco, Mexico City 07360.

[2] Pharmacology Department. Center for Research and Advanced Studies of the National Polytechnic Institute (CINVESTAV-IPN), Zacatenco Unit. 2508 National Polytechnic Institute Avenue. San Pedro Zacatenco, Mexico City 07360.

* Correspondence: cperezc@cinvestav.mx; Tel.: +52 (55) 5747 3800 Ext. 5442.

† Presented at the 1st International Electronic Conference on Microbiology, 2–30 November 2020; Available online: https://ecm2020.sciforum.net/.

Published: 02 November 2020

Graphical abstract:

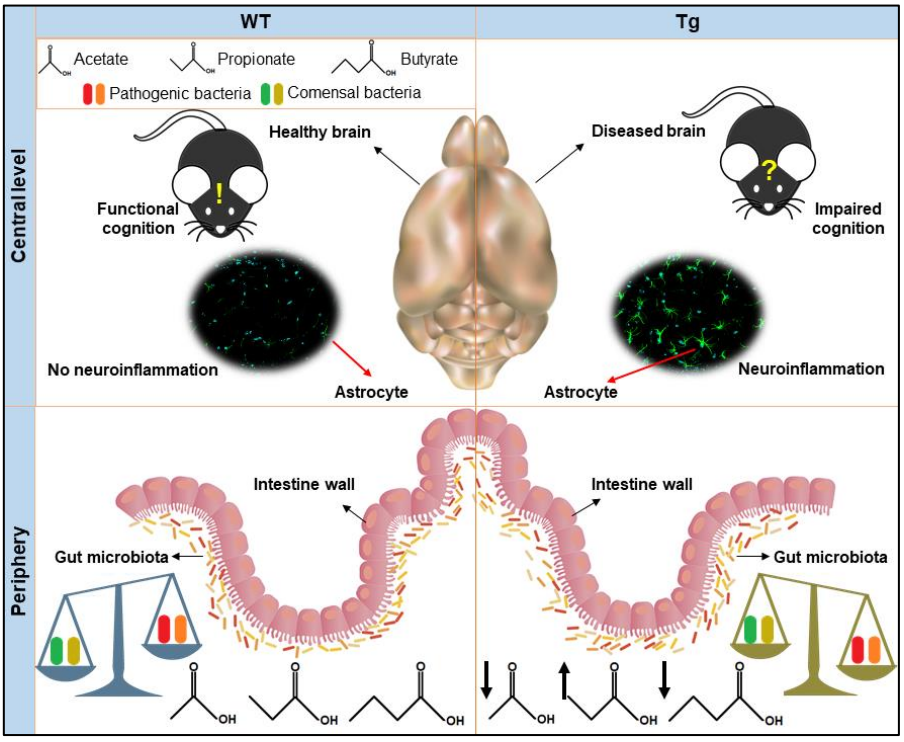

Abstract: Alzheimer´s disease (AD) is the most common age-related dementia. Recent investigations report gut-dysbiosis in transgenic (Tg) AD animals compared to wild type (WT) controls. Gut microbiota (GM)-produced propionate causes neuroinflammation, while butyrate possesses anti-inflammatory actions. The aim of the study was to determine whether the perturbations in GM were associated with short chain fatty acids (SCFAs) concentration in feces, and with cognitive impairment in AD-Tg mice. Six months-old WT and Tg male mice were evaluated for working- and spatial-memory performance by T- and water-maze, respectively.

Number of astrocytes was quantified in hippocampus and entorhinal cortex. SCFAs (acetate, propionate, and butyrate) fecal concentration was determined by chromatography, GM-related changes by DNA sequencing and bioinformatics. Our results showed that Tg mice presented working- and spatial-memory impairments, and astrogliosis in hippocampus compared to WT mice. Tg mice presented an enrichment of *Lactobacillus* genera and lower levels of acetate and butyrate compared to WT mice. Bioinformatics analysis suggested an increased propionate metabolism correlated with a higher propionate concentration in Tg mice in fecal samples. Our data suggests that GM dysbiosis leads to an enhanced propionate production in Tg mice, that might correlate with the neuroinflammation and cognitive impairment observed in these mice.

Keywords: Memory; astrocytes; acetate; butyrate; metabolism; transgenic; brain

1. Introduction

Alzheimer´s disease (AD) is a progressive neurodegenerative condition characterized by memory impairment and cognitive decline [1]. The histopathological diagnosis is based on the presence of amyloid plaques, and neurofibrillary tangles in the brain [2]. Today, no treatment is yet available to halt or reverse AD [3]. Recent reports highlight neuroinflammation as a key factor that contributes to the pathogenesis of AD, rather than plaques and/or tangles, themselves [4]. Disturbances in gut microbiota (GM), known as dysbiosis [5], has been also observed in AD patients [6]. Moreover, the short chain fatty acids (SCFAs) propionate and butyrate, produced by GM [7], have pro- [8] and anti-inflammatory [9] effects, respectively, not to mention that acetate is able to consolidate weak learning and rescue amyloid-impaired memory [10]. So, the objective of this work was to assess if GM dysbiosis could be associated with the concentration of fecal SCFAs, neuroinflammation and cognitive decline in a transgenic (Tg) murine model of AD.

2. Materials and Methods

Hemizygous amyloid precursor protein/presenilin 1 (APP/PS1) male mice (Tg, n=8) and their wildtype littermates (WT, n=9) of 6 months of age were used. One-week before sacrifice, behavioral testing was performed. Spontaneous alternations were quantified by T-maze (TM) as a directly proportional value of working memory, as specified by Deacon [11], while latency (time spend to find a platform hidden by the water level) was determined by water maze (WM) as an inversely proportional value of spatial learning through 12 consecutive trials, and spatial memory by a final trial without hidden platform as specified by Nunez [12]. Fecal samples were collected in clean cages and stored at -70ºC until use. Brains were immediately dissected out after sacrifice and post-fixed in 4 % paraformaldehyde (PFA) for 72 h at 4ºC. Brain tissue was cryoprotected by 30 % sucrose/water for 3 days. Coronal brain slices (40 μm thickness) from Bregma -1.94 mm to Bregma -2.18 mm were obtained for immunofluorescence (IF) [13], and stored at -20ºC until use. Brains sections were washed in PBS overnight and pre-treated 1 % $NaBH_4$ (Aldrich No. 19,807-2) at room temperature for 5 min, washed with distilled water and permeabilized with 0.5 % PBS-tween (PBSt) for 6 min, exposed to blocking solution [14] for 30 min at room temperature, incubated with the primary antibody (anti-glial fibrillary acidic protein, GFAP; [14], 1:1000 Abcam Cat. No. Ab53554) diluted in antibody signal enhancer solution [14] during 48 h at 4ºC, washed with 0.5 % PBSt, incubated with the secondary antibody (ALEXA647-conjugated anti-goat; [14] Jackson ImmunoRes Cat. No. 705-605-147) and 1.5 % donkey serum in 0.1 % PBSt at room temperature for 2 h, washed with 0.5 % PBSt, and finally, incubated with 4', 6-Diamidino-2-Phenylindole Dihydrochloride (DAPI; Invitrogen Cat. No. D1306, 1:500) in 0.1 % PBSt for 30 min, washed again with 0.5 % PBSt and mounted on glass slides using Vecta shield (Vector Laboratories). GFAP+ astrocytes were imaged by a confocal microscope (Leica TCSSP8) with argon (488 nm), and helium/neon (543 nm) lasers. GFAP+ astrocytes were quantified using the Fiji v. 1.46 plugin "analyze particles" in dentate gyrus, *stratum* (*st.*) *radiatum* and *st. oriens*

of CA1 hippocampal region, and layers I-VI from entorhinal Cx using a 40× objective performing optical scanning each 0.5 μm in Z axis.

To analyzed SCFAs concentration, at least 50 mg of $CaCO_3$ dried feces were suspended in 1 ml of deionized water by vortex mixing for 10 min, and centrifuged at 13000 rpm for the same time. The supernatant was processed through activated C-18 max 100 mg/mL GracePure™ Reversed-Phase SPE Columns according to the manufacturer's instructions. SCFAs were eluted with 1 mL of filtered water and analyzed via high performance liquid chromatography (HPLC) using 20:80 C_2H_3N:NaH_2PO_4 (pH=2.2 using H_3PO_4) as mobile phase as specified by De Baere [15]. Standard curves were prepared for acetate (Sigma-Aldrich No. 45754-100ML-F), propionate (Sigma-Aldrich No. P1386-500ML), and butyrate (Sigma-Aldrich No. B103500-500ML). On the other hand, bacterial DNA of fecal samples was extracted using the FavorPrep™ Stool DNA Isolation Mini Kit. Genomic libraries of 16S rDNA 3rd hypervariable region (V3) amplicons were generated, and massive sequencing was performed for each experimental subject as described by Corona-Cervantes [16]. Sequence alignments were done against the Greengenes 13.9 core set and microbiome analysis by QIIME software v1.9.0. Linear discriminant analysis (LDA) effect size (LefSe) program v1.0 was used to perform LDA (scores ≥ 2) to estimate the effect size of each bacterial taxa between groups [17]. Phylogenetics Investigation of Communities by Reconstruction of Unobserved States (PICRUSt) v.1.1.1 was used to predict metabolic profiles from 16S rDNA gene data set by Kyoto Encyclopedia of Genes and Genomes (KEGG) database at hierarchy level 3 pathways [18].

Data are expressed as the mean ± standard deviation (SD). Differences in the values of spontaneous alternations, WM latencies, SCFA concentration and proportion, number of GFAP+ astrocytes and GM relative abundances between experimental groups were evidenced by unpaired t-test followed by two-tailed test. Behavior learning curves were analyzed by a two-way repeated measure ANOVA followed by Tukey´s range test. Differences for taxa enrichment and predicted metabolic pathways were evidenced by LefSe and unpaired equal-variance t-test respectively. All results were considered statistically significant at $p < 0.05$.

3. Results

Working memory and spatial learning decreased in Tg compared to WT mice, with no significant changes in spatial memory (Figure 1). The number of GFAP+ astrocytes increased in hippocampus (dentate gyrus, *st. radiatum*, *st. oriens*) of Tg compared to WT mice, with no significant differences in entorhinal cortex (Figure 2). Tg mice presented an enhanced concentration and proportion of propionate, while acetate and butyrate proportions were decreased compared to WT mice (Table 1). Tg mice presented an increase of *Lactobacillus* and a decrease of Lachnospiraceae compared to WT mice. (Figure 3a). LEfSe analysis showed 10 and 9 enriched bacterial taxa for WT and Tg subjects respectively (Figure 3b). Finally, PICRUSt analysis showed 6 predictive metabolic pathways that differed significantly between experimental groups. Propanoate, pyruvate, arachidonic acid metabolism and diabetes mellitus type I were increased in Tg mice, while insulin signaling pathway, and Phe, Tyr and Trp biosynthesis were decreased compared to WT mice (Figure 4).

3.1. Figures, Tables and Schemes.

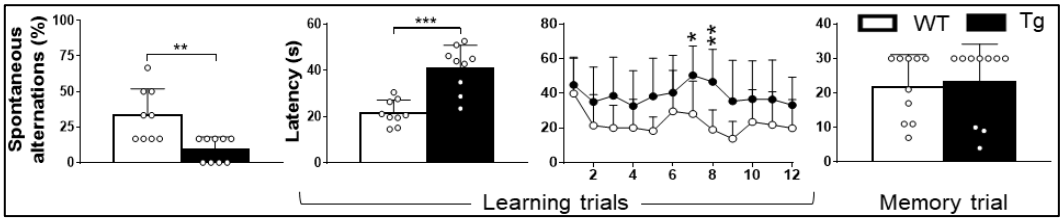

Figure 1. Cognitive performance. From left to right: working memory as a directly proportional value to spontaneous alternations in the TM, spatial learning average, spatial learning curves and spatial

memory as an inversely proportional value to the latency in the WM. Statistical significances for WT vs Tg mice are shown as *p < 0.05, **p < 0.01 and ***p < 0.001.

Table 1. Concentration and proportion of SCFAs in feces.

Unit	Group	Acetate	Propionate	Butyrate
µg/g	WT	24776.47	3056.42	2639.47
	Tg	14939.03*↓	9765.39**↑	1623.90
%	WT	80.34	9.30	10.36
	Tg	55.80***↓	37.56***↑	6.64**↓

Statistical significances for WT vs Tg mice are shown as *p < 0.05, **p < 0.01 and ***p < 0.001 per unit after numerical values for Tg animals. ↓: Decreased and ↑: Increased compared to WT mice.

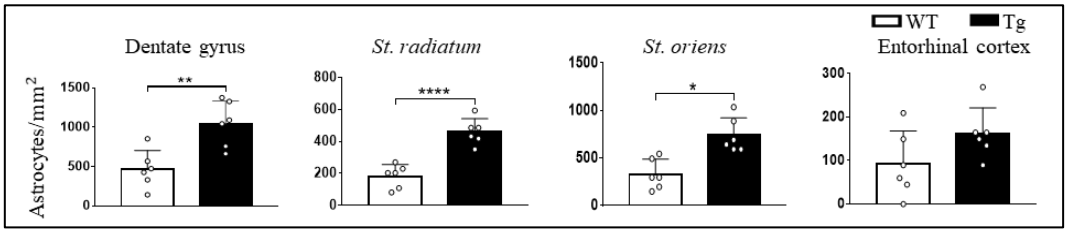

Figure 2. Neuroinflammation. GFAP+ astrocytes/mm² for different brain areas. Statistical significances for WT vs Tg mice are shown as *p < 0.05, **p < 0.01 and ***p < 0.001.

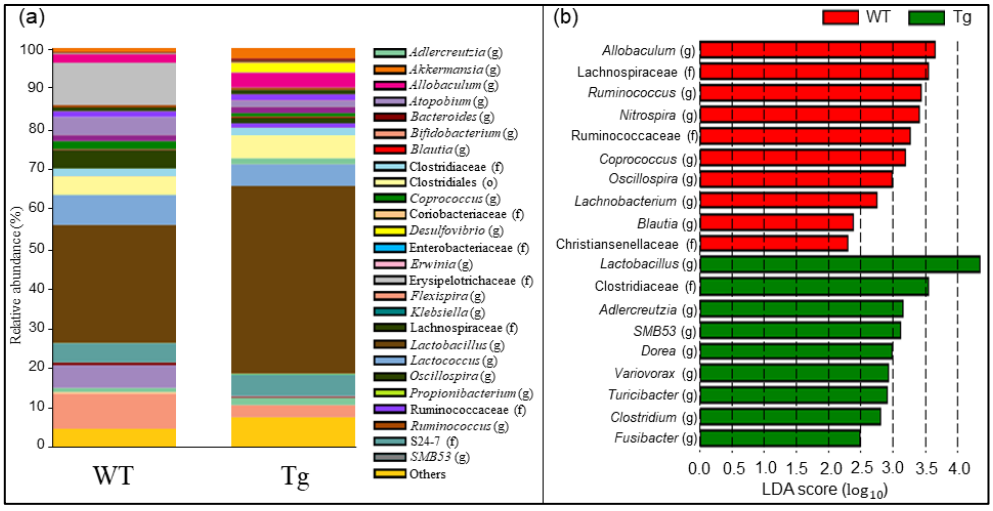

Figure 3. Relative abundance and enrichment of bacterial taxa. (**a**) Relative abundance of bacterial taxa. (**b**) LEfSe comparison of differentially abundant bacterial taxa associated with WT and Tg mice. LDA score cutoff of 2 was used to discriminate bacterial taxa. o: Orders, f: Families and g = Genera.

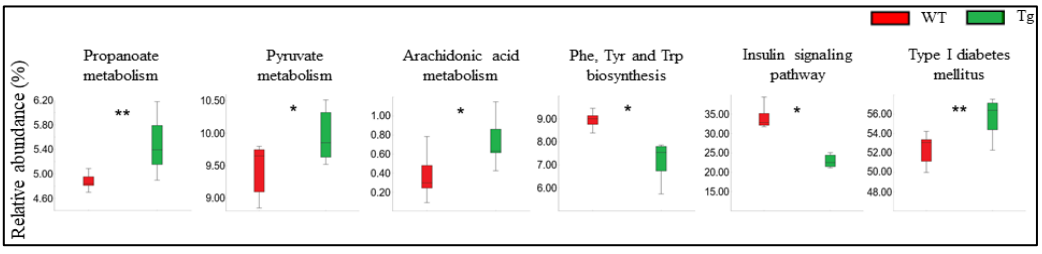

Figure 4. Prediction of the functional metagenome of the fecal bacterial microbiota. Graphic representations of significant predicted metabolic pathways determined by PICRUSt.

4. Discussion

We used 6 months-old APP/PS1 mice, as at this Tg mice present cognitive impairment [19], GM alterations [20], and GFAP-related neuroinflammation [21]. Therefore, this Tg mice model was ideal to demonstrate the impact of gut dysbiosis in SCFAs production and brain dysfunction. Our data confirm that 6 months-old Tg mice had working memory and spatial learning impairments compared to their WT mice (Figure 1). This Tg mice, also presented increased neuroinflammation in the hippocampal formation compared to controls. Enhanced astrocyte activation (Figure 2) related to neuroinflammation has been already reported in APP/PS1 mice [22]. It has been suggested that neuroinflammation contribute to cognitive impairment and neurodegenerative diseases [23]. We found an enhanced propionate concentration (a pro-inflammatory substance for astrocytes [8]), and a reduced butyrate concentration (anti-inflammatory [9]) in fecal samples of Tg mice (Table 1), that well correlate with the strong astrogliosis in AD mice. GM analysis indicated an increased relative abundance of *Lactobacillus* in Tg mice (Figure 3). This has been previously described in 2 months-old APP/PS1 mice [24], and in other AD models [25], even in human patients of AD [26]. *Lactobacillus* is a propionate producing bacteria, as already demonstrated for *L. buchneri*, *L. diolivorans*, *L. acidophilus*, *L. helviticus, L. rhamnosus* and *L. gasseri* [27, 28 and 29] species. This could well explain the enhanced propionate concentration in fecal samples of Tg mice (Table 1). Tg mice also presented a reduced concentration of acetate and butyrate compared to WT mice (Table 1), associated with a decreased abundance of butyrate producing bacteria, such as *Lachnospiraceae, Ruminococcaceae*, *Oscillospira*, as well as the acetate producers *Allobaculum, Blautia* and Christiansenellaceaea [30, 31, 32, 33 and 34], taxa that were enriched in fecal samples of the WT mice (Figure 3). Propanoate, pyruvate and arachidonic acid metabolism predictive pathways were found to be enhanced in Tg mice (Figure 4), in association with an enrichment of propionate producers [27, 28 and 29], and pyruvate [35] and arachidonic acid [36] metabolizers for this group. We observed increased neuroinflammation in the hippocampal formation of Tg mice, and arachidonic acid has been linked with an inflammatory response [36] that well correlate with our results. Type I diabetes mellitus metabolic pathways were increased in Tg mice, and a reduced insulin signaling pathway has been reported this mice model (Figure 4). mTOR signaling (involved in the mechanism of the insulin) can be modulated through *Lactobacillus* species [37 and 38]. Lower predicted values for Phe, Tyr and Trp biosynthesis in Tg mice (Figure 4) could be associated with the lower proportion of Clostridiales taxa (positively correlated with Phe, Tyr and Trp metabolism [39]). Moreover, low levels of Tyr and Phe have been associated with impaired processing during working memory performance [40] and reduced Phe, Tyr and Trp levels are found in AD patients compared to control individuals [41]. Therefore, our data suggest that working memory and spatial learning impairment is associated with GM-enhanced propionate production. Modulating SCFAs production by the GM [42] can be a strategy to ameliorate neuroinflammation and the cognitive impairment in AD.

5. Conclusion

Our data indicate that the increase in propionate concentration, and the reduction of acetate levels and butyrate proportion in Tg mice are associated with gut *Lactobacillus* enrichment. This can be associated with the increased neuroinflammation and the cognitive impairment in Tg mice compared to their WT controls.

Author Contributions: Conceptualization, CP-C and JG-M; methodology, AP-E, VS-Z, MI-F and DC-Z; software, MI-F and DC-Z; validation, MI-F and DC-Z; formal analysis, DC-Z; investigation, DC-Z; resources, J-GM and CP-C; data curation, AP-E, VS-V, MI-F and DC-Z; draft preparation, DC-Z; review and editing, JG-M, CP-C and DC-Z; visualization, DC-Z; supervision, JG-M and CP-C; project administration, JG-M and CP-C; funding acquisition, JG-M and CP-C.

Funding: This research was funded by SEP-CINVESTAV, and CONACyT grant numbers 163235 INFR-2011-01 and A1- S- 42600.

Acknowledgments: Thanks to CONACyT for Doctoral Fellowship to Daniel Cuervo-Zanatta (288396), Loan Edel Villalobos-Flores for bioinformatics counseling and Fernando Hernández-Quiroz for HPLC advising. JG-M (19815) and CP-C (47399) are Fellows from the Sistema Nacional de Investigadores, Mexico.

Conflicts of Interest: The authors declare no conflict of interest.

References

1. DeTure, M.A. and Dickson, D.W. The neuropathological diagnosis of Alzheimer's disease. *Mol. Neurodegener.* **2019**, *14*, 32.
2. Drummond, E., et al. Isolation of Amyloid Plaques and Neurofibrillary Tangles from Archived Alzheimer's Disease Tissue Using Laser-Capture Microdissection for Downstream Proteomics. *Methods Mol. Biol.* **2018**, *1723*, 319–334.
3. Malik, G. A. and Robertson, N. P. Treatments in Alzheimer's disease. *J. Neurol.* **2017**, *264*, 416–418.
4. Heneka, M.T., at al. Neuroinflammation in Alzheimer's disease. *Lancet Neurol*. **2015**, *14*, 388-405.
5. Toor, D., et al. Dysbiosis Disrupts Gut Immune Homeostasis and Promotes Gastric Diseases. *Int. J. Mol. Sci.* **2019**, *20*, 2432.
6. Kowalski, K. and Mulak, A. Brain-Gut-Microbiota Axis in Alzheimer's Disease. *J. Neurogastroenterol. and Motil.* 2019, *25*, 48–60.
7. Silva, Y. P., et al. The Role of Short-Chain Fatty Acids From Gut Microbiota in Gut-Brain Communication. *Front. Endocrinol*. **2020**, *11*, 25.
8. MacFabe, D. F. Enteric short-chain fatty acids: microbial messengers of metabolism, mitochondria, and mind: implications in autism spectrum disorders. *Microb. Ecol. Health Dis*. **2015**, *26*, 28177.
9. Kanski, R. S., et al. Histone acetylation in astrocytes suppresses GFAP and stimulates a reorganization of the intermediate filament network. *J Cell Sci*. **2014**, *127*, 4368-4380.
10. Gibbs, M.E., et al. Rescue of Abeta (1-42)-induced memory impairment in day-old chick by facilitation of astrocytic oxidative metabolism: implications for Alzheimer's disease. *J Neurochem*. **2009**, *109*, 230-236.
11. Deacon, R.M. and Rawlings, J.N. T-maze alternation in the rodent. *Nat Protoc*. **2006**, *1*, 7-12.
12. Nunez J. Morris Water Maze Experiment. *JoVE*. **2008**, *19*, 897.
13. Paxinos G., and Franklin, K.B.J. *The mouse brain: In Stereotaxic Coordinates.* 2nd ed.; Academic Press: San Diego, CA. United States of America, **2001**, pp. 47–49.
14. Rodríguez-Callejas, J. D., et al. Loss of ferritin-positive microglia relates to increased iron, RNA oxidation, and dystrophic microglia in the brains of aged male marmosets. *Am J Primatol*. **2019**, *81*, e22956.
15. De Baere, S., et al. Development of a HPLC-UV method for the quantitative determination of four short-chain fatty acids and lactic acid produced by intestinal bacteria during in vitro fermentation. *J Pharm Biomed Anal*. **2013**, *80*, 107–115.
16. Corona-Cervantes, K., et al. Human milk microbiota associated with early colonization of the neonatal gut in Mexican newborns. *PeerJ*. **2020**, *8*, e9205.
17. Segata, N., et al. Metagenomic biomarker discovery and explanation. *Genome Biol*. **2011,** *12*, R60.
18. Langille, M. G. et al. Predictive functional profiling of microbial communities using 16S rRNA marker gene sequences. *Nat Biotechnol*. 2013 *31*, 814–821.
19. Zhang, X., et al. Treadmill Exercise Decreases Aβ Deposition and Counteracts Cognitive Decline in APP/PS1 Mice, Possibly *via* Hippocampal Microglia Modifications. *Front Aging Neurosci*. **2019**, *11*, 78.
20. Bäuerl, C., et al. Shifts in gut microbiota composition in an APP/PSS1 transgenic mouse model of Alzheimer's disease during lifespan. *Lett Appl Microbiol*. **2018**, *66*, 464–471.
21. Radde, R., et al. Abeta42-driven cerebral amyloidosis in transgenic mice reveals early and robust pathology. *EMBO Rep*. **2006**, *7*, 940–946.
22. Abbink, M.R., et al. Characterization of astrocytes throughout life in wildtype and APP/PS1 mice after early-life stress exposure. *J Neuroinflammation*. **2020**, *17*, 91.
23. Zhao, J., et al. Neuroinflammation induced by lipopolysaccharide causes cognitive impairment in mice. *Sci Rep.* **2019**, *9*, 5790.
24. Xin, Y., et al. Effects of Oligosaccharides From *Morinda officinalis* on Gut Microbiota and Metabolome of APP/PS1 Transgenic Mice. *Front. Neurol*. **2018**, *9*, 412.
25. Bostanciklioğlu M. The role of gut microbiota in pathogenesis of Alzheimer's disease. *J Appl Microbiol*. **2019**, *127*, 954–967.
26. Zhuang, Z. Q., et al. Gut Microbiota is Altered in Patients with Alzheimer's Disease. **2018**, *JAD*, *63*, 1337–1346.
27. LeBlanc, J. G., et al. Beneficial effects on host energy metabolism of short-chain fatty acids and vitamins produced by commensal and probiotic bacteria. *Microb Cell Fact*. **2017**, *16*, 79.

28. Ong, L. and Shah, N.P. Influence of probiotic Lactobacillus acidophilus and L. helveticus on proteolysis, organic acid profiles, and ACE-inhibitory activity of cheddar cheeses ripened at 4, 8, and 12 degrees C. *J Food Sci*. **2008**, *73*, M111-M120.
29. Zhang, C., et al. Propionic acid production by cofermentation of Lactobacillus buchneri and Lactobacillus diolivorans in sourdough. *Food Microbiol*. **2010**, 27, 390-395.
30. Gophna, U., et al. Oscillospira and related bacteria - From metagenomic species to metabolic features. *Environ Microbiol*. **2017**,*19*, 835-841.
31. Herrmann, E., et al. RNA-Based Stable Isotope Probing Suggests *Allobaculum* spp. as Particularly Active Glucose Assimilators in a Complex Murine Microbiota Cultured In Vitro. *Biomed Res Int*. **2017**, 1829685.
32. Liu, C., et al. Influence of glucose fermentation on CO_2 assimilation to acetate in homoacetogen Blautia coccoides GA-1. *J Ind Microbiol Biotechnol*. **2015**, *42*, 1217-1224.
33. Vital, M., et al. Colonic Butyrate-Producing Communities in Humans: an Overview Using Omics Data. *mSystems*. **2017**, *2*, e00130-17.
34. Waters, J.L. and Ley, R.E. The human gut bacteria Christensenellaceae are widespread, heritable, and associated with health. *BMC Biol*. **2019**, *17*, 83.
35. Liu, S.Q. Practical implications of lactate and pyruvate metabolism by lactic acid bacteria in food and beverage fermentations. *Int J Food Microbiol*. **2003**, *83*, 115-131.
36. Bennett, P.R., et al. Preterm labor: stimulation of arachidonic acid metabolism in human amnion cells by bacterial products. *Am J Obstet Gynecol*. **1987**, *156*, 649-55.
37. Taherian-Esfahani, Z., et al. *Lactobacilli* Differentially Modulate mTOR and Wnt/ β-Catenin Pathways in Different Cancer Cell Lines. *Iran J Cancer Prev.* **2016**, *9*, e5369.
38. Mao, Z. and Zhang, W. (2018). Role of mTOR in Glucose and Lipid Metabolism. *Int J Mol Sci*. **2018**, *19*, 2043.
39. Elsden, S.R., et al. The end products of the metabolism of aromatic amino acids by Clostridia. *Arch Microbiol*. **1976**, *107*, 283-288.
40. Linssen, A.M., et al. Effects of tyrosine/phenylalanine depletion on electrophysiological correlates of memory in healthy volunteers. *J Psychopharmacol*. **2011**, *25*, 230-238.
41. Van der Velpen, V., et al. Systemic and central nervous system metabolic alterations in Alzheimer's disease. *Alzheimers Res Ther*. **2019**, *11*, 93.
42. Romo-Araiza, A. and Ibarra, A. Prebiotics and probiotics as potential therapy for cognitive impairment. *Med Hypotheses*. 2020, 134, 109410.